

# One-body reduced density matrix functionals for the homogeneous electron gas

N. N. Lathiotakis, N. Helbig, and E. K. U. Gross

*Institut für Theoretische Physik, Freie Universität Berlin,*

*Arnimallee 14, D-14195 Berlin, Germany*

## Abstract

A setback of the first generation functionals of the one-body reduced density matrix (1-RDM) is their failure to give a satisfactory approximation of the correlation energy of the homogeneous electron gas. Recently, new functionals of the 1-RDM were introduced, describing very accurately the cohesion and dissociation of diatomic molecules. We apply these functionals to the case of the HEG and show that the calculated correlation energy is significantly improved. Additionally, we introduce new functionals by fitting adjustable parameters to reproduce the exact correlation energy of the HEG.

PACS numbers: 71.10.-w,71.10.Ca,05.30.Fk,31.25.-v

## I. INTRODUCTION

Reduced density matrix functional theory (RDMFT) is one possible way to treat electronic correlations. It is based on Gilbert’s theorem [1], which is an extension of the Hohenberg-Kohn theorem to non-local external potentials. It guarantees that the expectation value of any observable of a system in its ground-state is a unique functional of the ground-state one-body reduced-density-matrix (1-RDM). Thus, the fundamental quantity in RDMFT is the 1-RDM instead of the electronic density on which DFT is built upon. The advantage of RDMFT, compared to DFT, is that the exact many-body kinetic energy is easily expressed in terms of the 1-RDM.

The properties of the exact 1-RDM functional have been the subject of theoretical studies for a long time [1, 2, 3]. The approximate functionals that have been introduced so far [4, 5, 6, 7, 8, 9, 10, 11, 12, 13, 14] are implicit functionals of the 1-RDM. They depend explicitly on the natural orbitals and the corresponding occupation numbers which are defined as the eigenfunctions and eigenvalues of the 1-RDM, respectively. The first such approximation was introduced by Müller [4] and it involves a total energy similar to Hartree-Fock. It differs, however, by the explicit inclusion of occupation numbers and a square root dependence on them in the exchange-like term. Actually, Müller considered a more general exponent for the occupation number product in the exchange-like term and found an optimal exponent of 1/2. By modeling the exchange and correlation hole, Buijse and Baerends [5] arrived at the same functional, while Goedecker and Umrigar [6] considered a modification by explicitly removing the self-interaction (SI) terms. Goedecker and Umrigar [6] also performed a direct minimization with respect to the natural orbitals and the occupation numbers. They found correlation energies for small atomic systems which are in very good agreement with the exact. However, it was found later that their functional fails to reproduce the correct dissociation limit for small molecules [15, 16]. On the other hand, the original Müller functional yields the correct dissociation limit but, in all cases, overestimates the correlation energy [15, 16].

Given the relative success of the Müller functional for small atoms and molecules, it was also applied to the homogeneous electron gas (HEG), which is another prototype system for testing new functionals. Cioslowski and Pernal [17] employed the Müller functional and

calculated analytically the momentum distribution  $n(k)$  of the HEG:

$$n(k) = 512\pi\rho (1 + 4k^2)^{-4}, \quad (1)$$

where  $\rho$  is the electron-density-per-spin,  $\rho = 3(8\pi r_s^3)^{-1}$ , and  $r_s$  is the radius (in atomic units) of the sphere with volume equal to the volume per electron. One can see that this fully variational solution is consistent with the  $N$ -representability constraint ( $0 \leq n(\mathbf{k}) \leq 1$ ) only for  $\rho \leq (512\pi)^{-1}$ , i.e.  $r_s \geq 5.77$ . The corresponding total energy per particle is independent of the density and equal to  $-1/8$  Hartree. In addition, Cioslowski and Pernal demonstrated that the Oxford-Lieb [18] bound is violated for  $\rho \geq 1.65 \times 10^{-3}$ , i.e.  $r_s \leq 4.167$ . Note that these two conditions are mutually exclusive. However, as demonstrated by Csányi and Arias [7], for  $r_s < 5.77$ , there is a momentum-distribution solution which is not fully variational. The momentum distribution is pinned to one for small wavevectors  $k$  due to the  $N$ -representability constraint and it is between zero and one for larger values of  $k$ . This behavior is also observed in finite systems, where the occupation numbers of the core states stay pinned to one. It is an essential feature of the Müller and Goedecker-Umrigar functionals. Unfortunately, the exact momentum distribution of the HEG [20, 21, 22] is strictly smaller than one, i.e. it is variational for the entire range of  $k$ . This feature of the exact solution is hence not reproduced by the Müller functional for  $r_s < 5.77$ .

In addition, Csányi and Arias [7] considered a functional, similar to that of Müller, derived from a tensor product expansion of the two-body density matrix, which they called Corrected Hartree Fock (CHF). Unfortunately, CHF gives zero correlation in the high density limit ( $r_s \rightarrow 0$ ) coinciding with Hartree-Fock. In the opposite limit i.e. for large  $r_s$  it strongly overcorrelates giving the same results as the Müller functional. In the intermediate region (metallic densities) the result for the correlation energy is close to the exact but its dependence on  $r_s$  is monotonically decreasing instead of increasing. In an attempt to improve over the Müller functional and CHF, Csányi, Goedecker and Arias considered an improved tensor product expansion of the two-particle density matrix [8]. The resulting functional, which is called CGA, performs very well in the high density regime and significantly better than the previous two functionals in the region of metallic densities. The deviation from the exact increases with  $r_s$  and at higher densities it coincides with CHF and the Müller functional.

In the last decade, several other functionals of the 1-RDM have been introduced [8, 9,

10, 11, 12, 13, 14] and exploited mainly in atomic and molecular calculations. Recently, Gritsenko et al. [13] proposed improved 1-RDM functionals based on a hierarchy of corrections to the Müller functional. These corrections, called BBC1, BBC2, and BBC3 make a distinction between strongly and weakly occupied orbitals and apply a series of corrections based on that distinction. The last correction, BBC3, involves additional corrections for the bonding and anti-bonding orbitals. All these functionals were constructed for optimizing the performance for finite systems. Gritsenko et al. [13] applied them to the dissociation of diatomic molecules and showed that they give an accurate description of these molecules at both the equilibrium distance and the dissociation limit.

In the present work, we apply the BBC1 and BBC2 functionals of Gritsenko et al. [13] to the HEG. The last of the corrections, BBC3, is not applicable to the HEG since it is based on corrections involving single orbitals. For the application of BBC1,2 one has to appropriately define the strongly and weakly occupied orbitals, since the corrections are based on that distinction. We choose a critical wavevector  $k_c$  which is equal to the Fermi wavevector,  $k_F$  of the non-interacting HEG, below which we consider the states to be strongly occupied. We find that the BBC1 functional gives results for the correlation energy which are closer to the exact than the original Müller functional. Applying the BBC2 correction in addition does not improve the results further.

An additional goal of this paper is to utilize the application of BBC functionals to the HEG in order to develop functionals suited for application to metallic systems. In order to achieve this goal we followed two different paths: First, we fit  $k_c$ , i.e. the critical wavevector for the distinction between weakly and strongly occupied orbitals, such that BBC1 reproduces the exact correlation energy of the HEG. We call this functional  $k_c$ -functional. Second, we keep  $k_c = k_F$  but adopt a fitting parameter  $s$  multiplying the exchange terms for two weakly occupied orbitals. In this way, we replace the sign change of the BBC1 functional with this parameter. Accordingly, we call this functional  $s$ -functional. To assess these two different paths, we use the agreement of the momentum distribution with the exact as a criterion. We show that the second, namely the  $s$ -functional, is superior, it reproduces the correlation energy of the HEG exactly, also giving reasonable results for the momentum distribution. Consequently, it is expected to be accurate in the description of electronic correlation in metallic systems.

This paper is organized as follows: In Section II we introduce RDMFT for the HEG

and review the BBC corrections. We also present the two new functionals in that Section. Details of the numerical implementation and the results are presented in Section III. We close this paper with concluding remarks in Section IV.

## II. RDMFT FOR THE HOMOGENEOUS ELECTRON GAS

Most of the functionals of the 1-RDM that have been introduced so far can be written in the general form

$$E_{\text{tot}} = \sum_i n_i \phi_i^*(\mathbf{r}) \left[ -\frac{\nabla^2}{2} + V_{\text{ext}}(\mathbf{r}) \right] \phi_i(\mathbf{r}) + \sum_{ij} n_i n_j \int \int \frac{\phi_i^*(\mathbf{r}) \phi_j^*(\mathbf{r}') \phi_i(\mathbf{r}) \phi_j(\mathbf{r}')}{|\mathbf{r} - \mathbf{r}'|} d^3 \mathbf{r} d^3 \mathbf{r}' - \sum_{ij} f(n_i, n_j) \int \int \frac{\phi_i^*(\mathbf{r}) \phi_j^*(\mathbf{r}') \phi_j(\mathbf{r}) \phi_i(\mathbf{r}')}{|\mathbf{r} - \mathbf{r}'|} d^3 \mathbf{r} d^3 \mathbf{r}', \quad (2)$$

where  $V_{\text{ext}}(\mathbf{r})$  is an external local potential like the attractive ion potential. The last term is exchange-like and the functional of Eq. (2) reduces to Hartree-Fock for  $f(n_i, n_j) = n_i n_j$ . For the Müller [4, 5] and Goedecker-Umrigar [6] functionals  $f(n_i, n_j) = \sqrt{n_i n_j}$ , but for the Goedecker-Umrigar functional the self-interaction terms are excluded from the direct Coulomb and the exchange-like terms. If we apply the above total energy expression (2) to the HEG then, as in the case of Hartree Fock, the direct Coulomb, the ion-electron and the ion-ion interaction terms cancel exactly. Only two terms survive, the kinetic and the exchange-like, and therefore the total energy is given by

$$E_{\text{tot}} = 2 \sum_{\mathbf{k}_1} \frac{\mathbf{k}_1^2}{2} n(k_1) - \frac{1}{V} \sum_{\mathbf{k}_1, \mathbf{k}_2} f(n(k_1), n(k_2)) \frac{4\pi}{|\mathbf{k}_1 - \mathbf{k}_2|^2 + \alpha^2}, \quad (3)$$

where  $\mathbf{k}_1, \mathbf{k}_2$  are wavevector indices and  $V$  is the volume of the system ( $V \rightarrow \infty$ ). The quantity  $n(k)$  is the momentum distribution, i.e. the occupation number of the state with wavevector  $\mathbf{k}$  and due to the spherical symmetry it depends only on the magnitude  $k$ . Following Csányi and Arias [7], we introduce a screening parameter  $\alpha$  in the exchange term, i.e. we assume a Yukawa rather than a pure Coulomb potential for numerical reasons.

Recently, improved functionals of the 1-RDM were introduced by Gritsenko et al. [13]. They are based on the distinction between strongly and weakly occupied states and consist of a hierarchy of corrections to the Müller functional.

The first correction, called BBC1, introduces a sign change of the function  $f(n(k_1), n(k_2))$  in Eq. (2) if both states,  $\mathbf{k}_1$  and  $\mathbf{k}_2$ , are weakly occupied, i.e.

$$f(n(k_1), n(k_2)) = \begin{cases} -\sqrt{n(k_1) n(k_2)}, & \text{both } \mathbf{k}_1, \mathbf{k}_2 \text{ weakly occupied,} \\ \sqrt{n(k_1) n(k_2)}, & \text{otherwise.} \end{cases} \quad (4)$$

The second correction in the hierarchy, BBC2, restores the exact exchange form for the last term in Eq. (2) if both states are strongly occupied, i.e.

$$f(n(k_1), n(k_2)) = \begin{cases} -\sqrt{n(k_1) n(k_2)}, & \text{both } \mathbf{k}_1, \mathbf{k}_2 \text{ weakly occupied,} \\ n(k_1) n(k_2), & \text{both } \mathbf{k}_1, \mathbf{k}_2 \text{ strongly occupied,} \\ \sqrt{n(k_1) n(k_2)}, & \text{otherwise.} \end{cases} \quad (5)$$

Finally, the third correction, BBC3, is applied on top of BBC2 and it includes the anti-bonding orbital in the list of 'strongly occupied orbitals', changing  $f$  accordingly, unless the pairing orbital is the bonding one. In addition, like in the Goedecker-Umrigar functional [6], the self-interaction terms are removed. Clearly, BBC3 is not applicable to the case of the HEG since the concept of bonding and anti-bonding orbitals is restricted to finite systems and the self-interaction is known to vanish in the thermodynamic limit ( $V$  going to infinity).

The minimization of the total energy of Eq. (2) with respect to  $n(k)$ , under the constraint of particle number conservation, can be done using the Lagrange-multipliers method. We introduce a Lagrange-multiplier  $\mu$ , resembling the chemical potential, and minimize the quantity  $F$

$$F = E_{\text{tot}} - \mu \left[ \frac{V}{(2\pi)^3} \int d^3 \mathbf{k}_1 n(k_1) - N \right]. \quad (6)$$

The angular integrations can be carried out analytically, like in the Hartree-Fock case, and we arrive at the following expression for  $F$  per particle

$$\begin{aligned} \frac{F}{N} = & \frac{3}{2k_F^3} \int_0^\infty dk_1 k_1^2 (k_1^2 - 2\mu) n(k_1) \\ & + \frac{3}{4\pi k_F^3} \int_0^\infty dk_1 \int_0^\infty dk'_2 k_1 k_2 \log \left[ \frac{(k_1 - k_2)^2 + \alpha^2}{(k_1 + k_2)^2 + \alpha^2} \right] f(n(k_1), n(k_2)) + \mu, \end{aligned} \quad (7)$$

where  $k_F = (9\pi/4)^{1/3} r_s^{-1}$  is the Fermi-wavevector of the non-interacting HEG. We now turn to the question of how to transfer the definition of strongly and weakly occupied states from finite systems to the HEG. We can define a critical wavevector  $k_c$  below which all

states are assumed to be strongly occupied while above they are weakly occupied. For finite closed-shell systems, Gritsenko et al. [13] chose the first  $N/2$  natural orbitals to be strongly occupied. For the HEG, the equivalent choice is  $k_c = k_F$ .

A different choice, which goes beyond BBC's towards the development of a new functional, is to treat  $k_c$  as an adjustable parameter. It is chosen such that the exact correlation energy of the HEG. As exact results for the correlation energy of the HEG, we regard the Perdew-Wang fit [19] for the correlation energy obtained from dynamic Monte-Carlo (DMC) calculations by Ceperley and Alder [20] and Ortiz and Ballone [21]. The two Monte-Carlo calculation yield almost identical correlation energies. Since  $k_c$  is fitted for every single value of  $r_s$  we considered, it becomes a function of  $r_s$ . In the present work, we apply this procedure to the BBC1 functional, and we call the resulting functional  $k_c$ -functional. The corresponding  $f$  function reads

$$f(n(k_1), n(k_2)) = \begin{cases} -\sqrt{n(k_1) n(k_2)}, & k_1, k_2 > k_c(r_s), \\ \sqrt{n(k_1) n(k_2)}, & k_1, k_2 < k_c(r_s). \end{cases} \quad (8)$$

An alternative idea is to keep  $k_c$  fixed and equal to  $k_F$  and consider a fitting parameter  $s$  multiplying the exchange-like terms when both states,  $\mathbf{k}_1$  and  $\mathbf{k}_2$ , are weakly occupied, i.e.

$$f(n(k_1), n(k_2)) = \begin{cases} -s(r_s) \sqrt{n(k_1) n(k_2)}, & k_1, k_2 > k_F, \\ \sqrt{n(k_1) n(k_2)}, & k_1, k_2 < k_F. \end{cases} \quad (9)$$

In this way, the parameter  $s$  which is a kind of strength of the exchange-like terms becomes a function of  $r_s$ , as indicated in Eq. (9). We call this functional the  $s$ -functional.

The criterion for the success of the above functionals is the resemblance of the resulting momentum distributions to the exact. We compare the momentum distributions we obtain with the fitting formulas of Ortiz and Ballone [21] and Gori-Giorgi and Ziesche [22] to the quantum Monte-Carlo results [21]. The exact momentum distribution is a monotonically decreasing function of  $k$  and always smaller than 1. It is concave for  $k < k_F$ , shows a discontinuity at  $k_F$ , and for  $k > k_F$  it goes to zero asymptotically. The size of the discontinuity is decreasing with  $r_s$ . In the next section, we present both the application of BBC1 and BBC2 corrections to the HEG, as well as the evaluation of the two new functionals.

### III. NUMERICAL IMPLEMENTATION, RESULTS

The minimization of the energy expression of Eq. (7) with respect to the momentum-distribution function  $n(k)$  is performed using the steepest descent method. We choose to work in the energy-space instead of  $k$ -space, i.e. we employed the variable substitution  $\epsilon = k^2/2$  and solved numerically the minimization problem for  $n(\epsilon)$ . Working in the energy-space rather than  $k$ -space improves the stability of the numerical treatment. The energy  $\epsilon$  is discretized using a double-logarithmic mesh centered in the area of interest, where the occupation varies the most. In most cases this area is around  $\epsilon_F = k_F^2/2$ . The upper limit of integration is chosen such that the momentum-distribution function has dropped to values smaller than  $10^{-6}$ . The double integration with respect to the energy is carried out using an adaptive grid technique capable of treating integrable singularities like the logarithmic singularity of the present problem. The values of the energy-distribution function  $n(\epsilon)$  in between the mesh points, necessary for the adaptive grid method, are obtained from an interpolation scheme. The  $N$ -representability constraint  $0 \leq n(\epsilon) \leq 1$  is implemented through the substitution  $n(\epsilon) = \sin^2[\pi \theta(\epsilon)/2]$  and varying with respect to  $\theta(\epsilon)$ . Extra care is required to avoid  $n(\epsilon)$  being falsely pinned to 0 or 1. Indeed, if for a particular  $\epsilon$ ,  $n(\epsilon)$  gets very close to 1 or 0 during the variation it will stay pinned at that point. The variation with respect to the Lagrange-multiplier  $\mu$  is implemented as an external iterative procedure, thus achieving convergence for each value of  $\mu$ . The correct value of  $\mu$  is selected by requiring the momentum-distribution function to integrate to the correct number of electrons for a given value of  $r_s$ . Finally, we found that a reasonable value for the parameter  $\alpha$  in Eq. (3) is  $10^{-8}$ , which avoids both numerical problems as well as the dependence of the results on  $\alpha$ .

#### A. Application of BBC's to the HEG

In Fig. 1, we show the correlation energy of the HEG as a function of  $r_s$ . The correlation energy calculated with the BBC1 and BBC2 functionals is significantly closer to the exact than any other functional over the whole range of  $r_s$ . Both functionals also seem to reproduce the correct asymptotic limit of zero correlation for the dilute HEG. For small densities and up to the metallic densities ( $r_s \sim 1$ ) the BBC functionals under-correlate. In the dense limit they over-correlate and the crossover is at around  $r_s=0.5$  and 0.3 for the BBC1 and

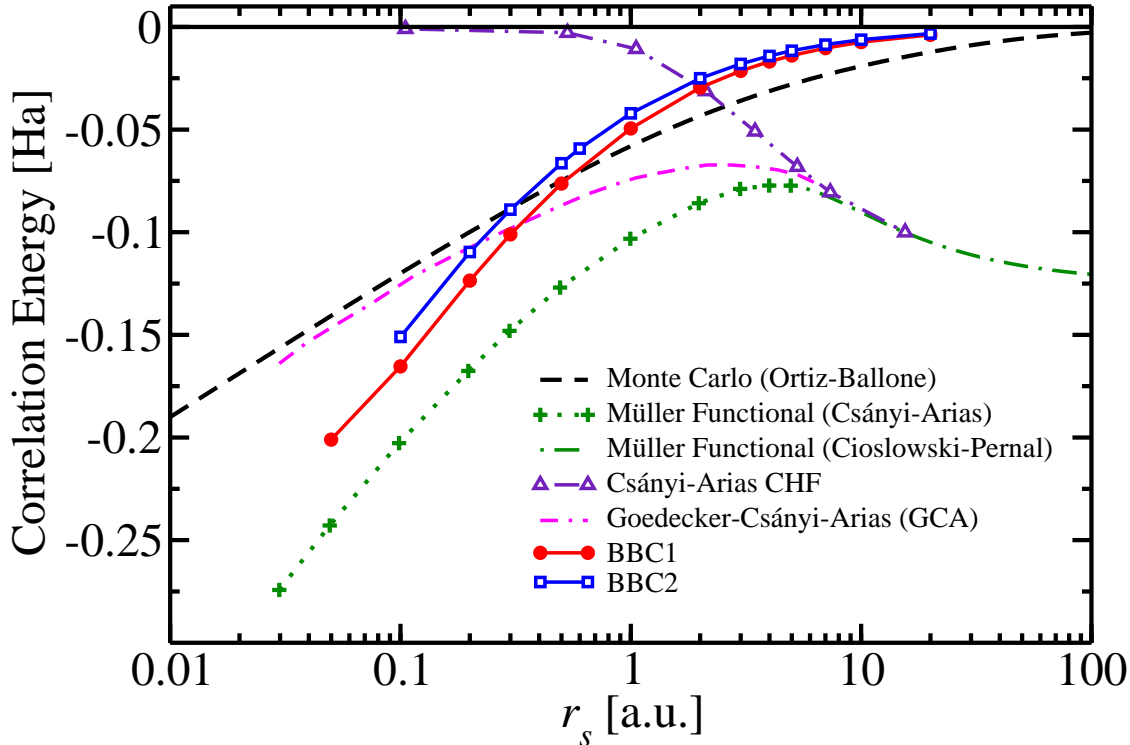


FIG. 1: The correlation energy of the HEG as a function of  $r_s$ . The dashed line corresponds to the Perdew-Wang fit [19] for the DMC data of Ortiz and Ballone [21]. The dotted line corresponds to the numerical results by Csányi and Arias [7] employing the Müller functional, for  $r_s < 5.77$ . Its continuation, the dash-dotted line for  $r_s > 5.77$ , stands for the analytical results of Cioslowski and Pernal [17] employing the same functional. The results for the CHF functional [7] as well as the CGA [8] are also shown with dashed-dotted line with triangles and double dashed-dotted line respectively. Finally, the continuous lines with the circles and the squares correspond to the present work using the BBC1 and BBC2 functionals, respectively.

BBC2, respectively. Unfortunately, in the area of low metallic densities both functionals yield correlation energies which deviate from the exact by 50%. In absolute numbers, the error of BBC1 and BBC2 is of the same order as the RPA result [19]. Nevertheless, in the range  $0.1 < r_s < 1$ , the BBC functionals perform remarkably well. Compared to all previous 1-RDM functionals, BBC1 and BBC2 offer a better account of the electron correlation for the HEG. Although less accurate than the CGA in the high density region, they perform better for metallic densities and they reproduce the limit of zero correlation at the dilute HEG limit where the Müller functional, CHF and CGA fail.

A feature of the exact momentum distribution, namely a discontinuity at the Fermi wavevector  $k_F$ , is reproduced by BBC functionals. So far, there is no report of any other 1-RDM functional reproducing this feature of the HEG. The discontinuity is more pronounced for the BBC1 functional, as can be seen in Fig. 2, where we plotted the momentum distribution of the HEG with  $r_s = 1$  and  $r_s = 5$  using the Müller functional as well as BBC1 and BBC2. To extract the size of the discontinuity, we used two energy mesh points very close to  $\epsilon_F$  (at a distance of  $10^{-8}\epsilon_F$ ). In Fig. 3, we plot the size of the discontinuity  $\Delta n$  as a function of  $r_s$ . As we see, it increases monotonically with  $r_s$  and has the tendency to saturate for large  $r_s$ . For BBC2 the discontinuity is substantially smaller than for BBC1 and it goes to zero at  $r_s$  around 0.6. Unfortunately, both the size and the dependence on  $r_s$  are in complete disagreement with the exact theory, where  $\Delta n$  is substantially bigger and decreases with  $r_s$ .

One of the features of the original Müller functional is that the momentum distribution is equal to 1 for small wavevectors  $k$ . For these wavevectors  $n(k)$  is determined by the  $N$ -representability constraint and therefore the solution is not variational ( $\delta(F/N)/\delta n(k) \neq 0$ ). We found that this feature is preserved in the BBC1 and BBC2 corrections. This can be seen in Fig. 2 where we also show the derivative  $\delta(F/N)/\delta n(k)$  as a function of  $k$ . For small  $k$  the derivative is negative indicating that, without the  $N$ -representability constraint,  $n(k)$  would increase beyond 1. Then, after a critical wavevector  $k_p$  the derivative is zero and the momentum distribution becomes smaller than one. In Fig. 4, we plot  $k_p$  as a function of  $r_s$ . For all functionals,  $k_p$  decreases monotonically with  $r_s$ . It was proven analytically that for the Müller functional, there is a critical value of  $r_s = 5.77$  above which the solution is fully variational [17]. As it is demonstrated in Fig. 4,  $k_p$  goes to zero at the same critical value for the Müller functional, in complete agreement with the analytical result. This can be also seen in Fig. 2, where for the Müller functional and  $r_s = 5$  (upper-right plot) the derivative is very close to zero even for small wavevectors. Interestingly, for BBC1 and BBC2 we found no such critical value up to  $r_s = 20$ . Indeed, for both BBC1 and BBC2 the decrease is much slower with  $k_p$  being almost constant for BBC2. We should mention that the behavior of  $n(k)$  for small wavevectors is in complete analogy to the behavior when the three functionals are applied to finite systems, where it is well documented that the occupation numbers of the core states are pinned to 1, due to the  $N$ -representability constraint.

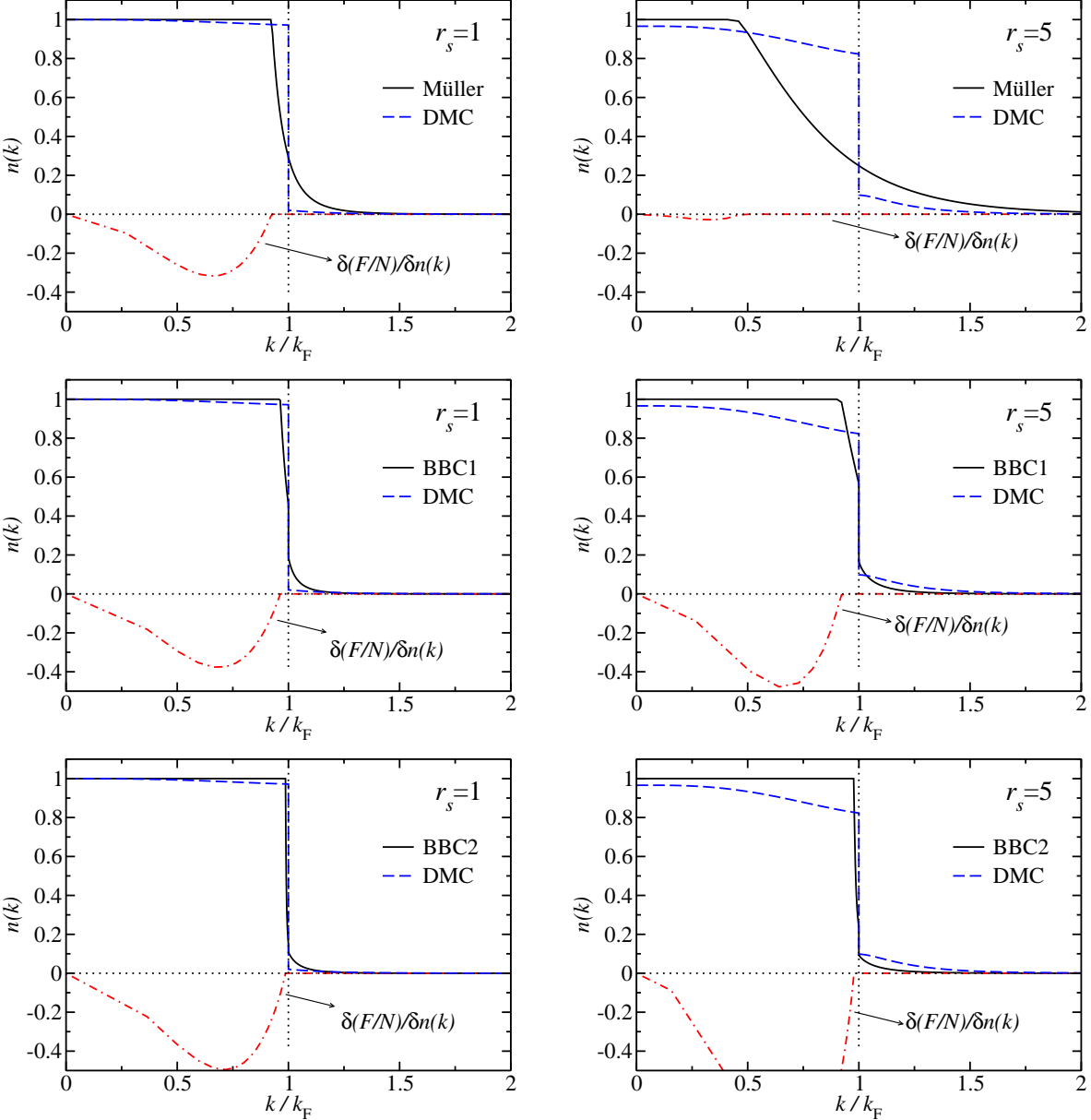


FIG. 2: The momentum distribution  $n(k)$  of the HEG for  $r_s=1$  (left) and  $r_s = 5$  (right) as calculated with the Müller functional, and the BBC1 and BB2 corrections. BBC1 and BBC2 show a discontinuity of the momentum distribution at  $k_F$ . For comparison we include the fit to the DMC data of Ortiz-Ballone [21]. The derivative  $\delta(F/N)/\delta n(k)$  is also plotted. Notice that for small  $k$  the derivative is not zero and  $n(k)$  is pinned to one.

### B. Improved functionals for the HEG

As already mentioned, we pursue two strategies to improve the performance of the BBC1 functional for the HEG. The goal is to develop a 1-RDM functional applicable to metallic

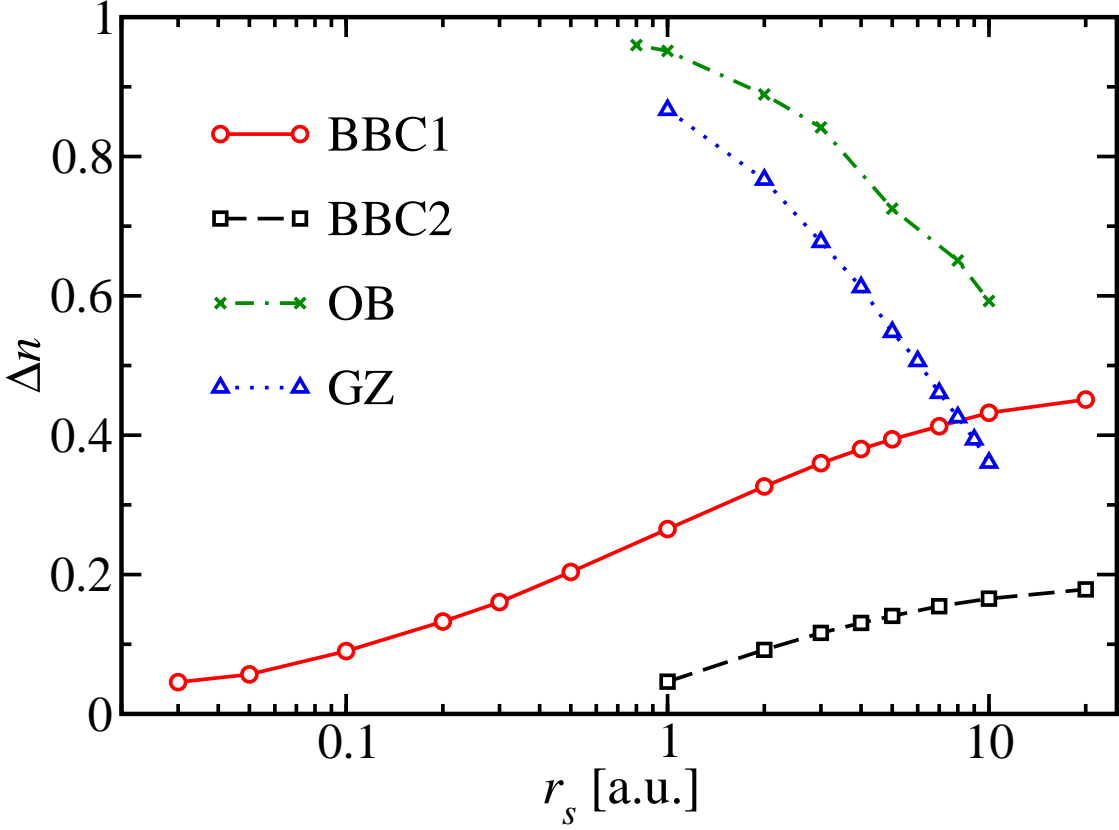


FIG. 3: The discontinuity  $\Delta n$  of the momentum distribution at  $k_F$  for BBC1 and BBC2 as a function of  $r_s$ , compared to the fit to the DMC data of Ortiz and Ballone (OB) [21], and Gori-Giorgi and Ziesche (GZ) [22].

$r_s$	0.5	1.0	2.0	3.0	4.0	5.0
$k_c/k_F$	1.0	1.032	1.085	1.122	1.155	1.172

TABLE I: The critical wavevector  $k_c$  for some metallic densities.

systems.

For the first functional, namely the  $k_c$ -functional, we fit the critical wavevector  $k_c$ , separating the strongly and weakly occupied states, such that the exact correlation energy of the HEG is reproduced. We perform this fitting on the basis of the BBC1 functional over the range of metallic densities,  $0.5 \leq r_s \leq 5$ . The results are compiled in Table I. Fitting  $k_c$  has a strong impact on the momentum distribution which is displayed in Fig. 5. It is not surprising that the discontinuity is displaced from  $k_F$  to  $k_c$ . Additionally, its size is reduced significantly compared to BBC1.

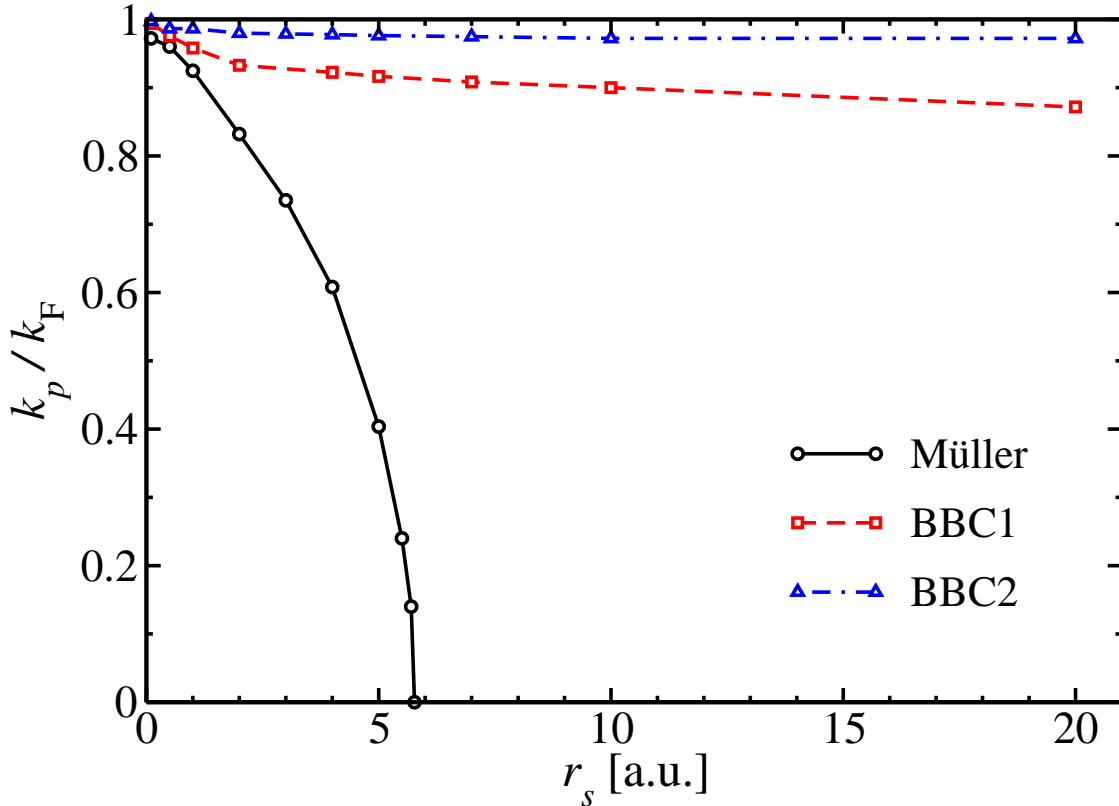


FIG. 4: The critical wavevector  $k_p$ , where the optimal momentum distribution becomes fractional, as a function of  $r_s$ .

The  $s$ -functional is also based on BBC1 but with  $k_c = k_F$ , and a fitting parameter  $s$  multiplying the exchange-like terms for two weakly occupied orbitals. It also reproduces the correct correlation energy for the HEG, for the whole range of  $r_s$ . For the fitting, we used two different sets of Monte-Carlo results: the Ceperley and Alder [20] and the Ortiz and Ballone [21]. The values of  $s$  for the fitting to the Ortiz and Ballone DMC results are included in TableII. As we see,  $s$  varies between 4 and  $-0.26$  for the range of densities ( $0.1 < r_s < 10$ ) we considered. The resulting function  $s(r_s)$  is shown in Fig. 6.

From Fig. 7 one can see that one of the advantages of fitting  $s$  instead of  $k_c$  is that the discontinuity of the momentum distribution remains fixed at  $k_F$ . In addition, its size is almost constant ( $\approx 0.2$ ) as a function of  $r_s$ . As we see in Fig. 3, the exact discontinuity is significantly higher and it is a decreasing function of  $r_s$ . Concerning the size of the discontinuity, the  $s$ -functional does not improve over the BBC1, since in the dilute gas limit the discontinuity given from BBC1 is closer to the exact. However, the increasing behavior

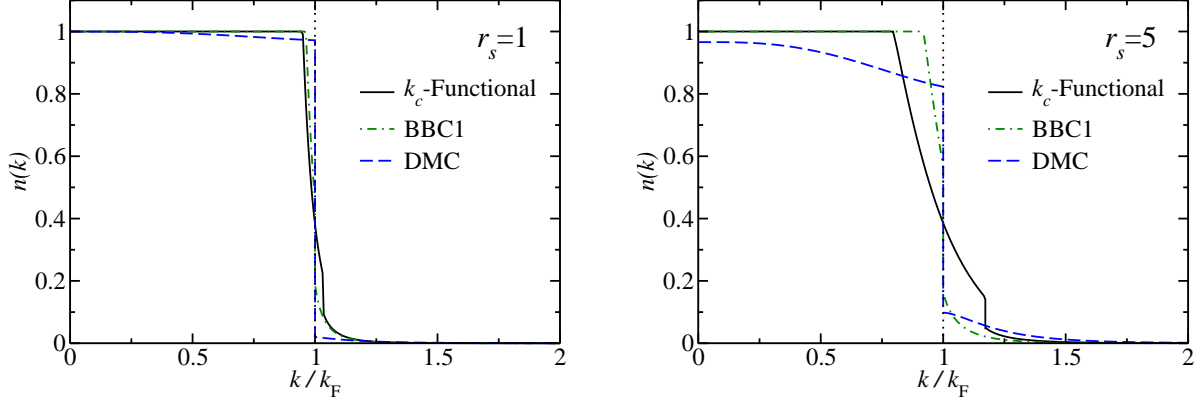


FIG. 5: The momentum distribution for the  $k_c$ -functional compared with the BBC1 and the fit to the DMC data of Ortiz-Ballone [21], for  $r_s = 1$  and  $r_s = 5$ . For the  $k_c$ -functional the discontinuity has moved from  $k_F$  to  $k_c = 1.032$  and  $k_c = 1.172k_F$  respectively.

$r_s$	$s$	$r_s$	$s$
0.1	4.913	1.0	0.435
0.2	2.751	1.5	0.190
0.3	1.867	2.0	0.059
0.4	1.390	3.0	-0.074
0.5	1.087	4.0	-0.146
0.6	0.877	5.0	-0.189
0.7	0.727	7.0	-0.234
0.8	0.602	10.0	-0.263

TABLE II: The fitted values of  $s$  for various values of  $r_s$  for the  $s$ -functional.  $s$  was fitted to reproduce the correlation energies of the DMC calculation of Ortiz and Ballone [21].

of BBC1 is improved by the  $s$ -functional which yield discontinuities almost constant.

#### IV. CONCLUSION

We apply revised 1-RDM functionals [13] to the HEG. We show that they offer a significant improvement over the Müller functional as far as the correlation energy is concerned. In addition, they yield a discontinuity of the momentum distribution at the Fermi wavevector in resemblance of the exact HEG theory. Unfortunately, the size and the dependence on the

density of this discontinuity are not in agreement with the quantum Monte-Carlo results.

By using an appropriate fitting parameter, we demonstrate that the exact correlation energy of the HEG can be reproduced. For this parameter, we either use the critical wavevector  $k_c$  which distinguishes between the strongly and weakly occupied states, or a strength  $s$  multiplying the exchange-like terms for two weakly occupied states. Both these procedures were applied to the BBC1 functional. The two new functionals, being exact as far as the correlation energy is concerned, are assessed by the quality of the resulting momentum distributions. We show that choosing the second procedure is superior to fitting  $k_c$ , and also improves the results of BBC1 and BBC2 significantly.

Our functional of choice, being derived from the HEG, is expected to yield good results for metallic systems. The application to finite as well as non-metallic periodic systems is complicated by the fact that  $r_s$  is not well defined. Therefore, one has to device methods to map  $r_s$  onto other quantities characterizing these systems. We are currently employing ideas in this direction.

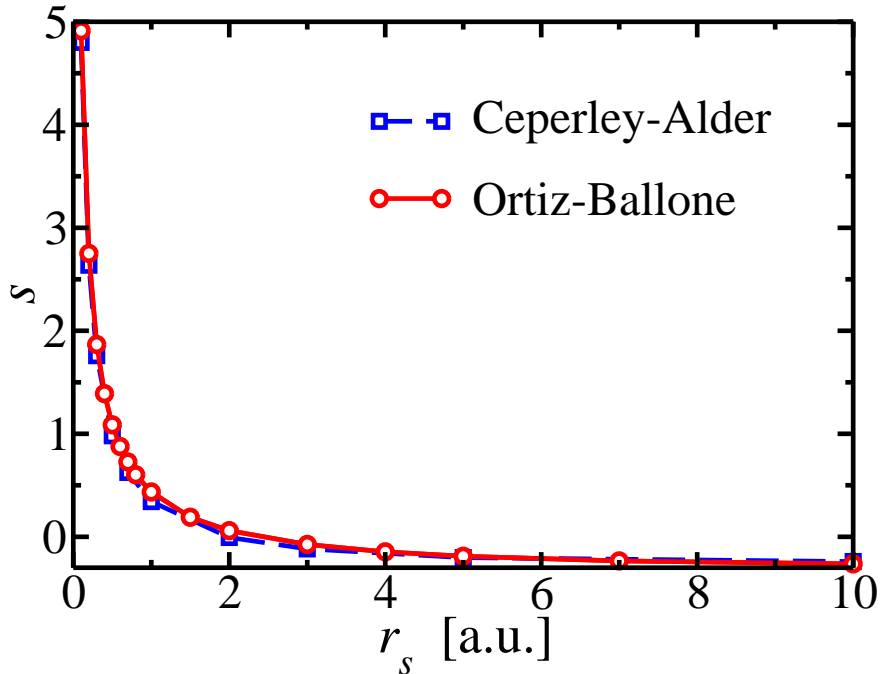


FIG. 6: The dependence of the fitting parameter  $s$  on  $r_s$ . The parameter  $s$  was obtained from the requirement that the functional reproduces the correlation energy of the Perdew Wang fit [19] to two different sets of DMC results: the Ceperley and Alder [20] and the Ortiz and Ballone [21].

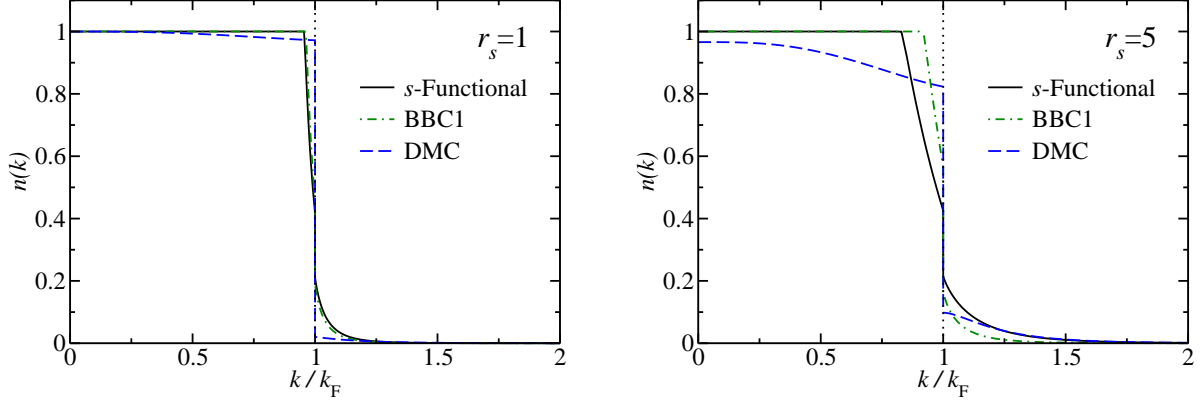


FIG. 7: The momentum distribution given by the  $s$ -functional, compared with the BBC1 and the fit to the DMC data of Ortiz-Ballone [21], for  $r_s = 1$  with  $s = 0.435$ , and  $r_s = 5$  ( $s = -0.189$ ). The discontinuity is fixed at  $k_F$  and is approximately equal to 0.2.

### Acknowledgments

This work was supported in part by the Deutsche Forschungsgemeinschaft within the program SPP 1145, by the EXCITING Research and Training Network, and by the NANOQUANTA Network of Excellence.

---

[1] T. L. Gilbert, Phys. Rev. B**12**, 2111 (1975).

[2] S. M. Valone, J. Chem. Phys. **73**, 1344 (1980); **73**, 4653 (1980).

[3] G. Zumbach and K. Maschke, J. Chem. Phys. **82**, 5604 (1985).

[4] A. M. K. Müller, Phys. Lett. A **105**, 446 (1984).

[5] M.A. Buijse, PhD Thesis, Vrije Universiteit Amsterdam (1991); M. A. Buijse, E. J. Baerends, Mol. Phys. **100**, 401 (2002).

[6] S. Goedecker, C. J. Umrigar, Phys. Rev. Lett. **81**, 866 (1998).

[7] G. Csányi, T. A. Arias, Phys. Rev. B**61** (2000) 7348.

[8] G. Csányi, S. Goedecker, T. A. Arias, Phys. Rev. A**65** 032510 (2002).

[9] K. Yasuda, Phys. Rev. Lett. **88**, 053001 (2002).

[10] C. Kollmar, J. Chem. Phys. **121**, 11581 (2004).

[11] J. Cioslowski, K. Pernal, M. Buchowiecki, J. Chem. Phys. **119**, 6443 (2003).

[12] K. Pernal, J. Cioslowski, J. Chem. Phys. **120**, 5987 (2004).

- [13] O. Gritsenko, K. Pernal, E. J. Baerends, *J. Chem. Phys.*, **122**, 204102 (2005).
- [14] J. Cioslowski and K. Pernal, *Phys. Rev. B* **71**, 113103 (2005).
- [15] V. N. Staroverov and G. E. Scuseria, *J. Chem. Phys.* **117**, 2489 (2002).
- [16] J. M. Herbert, J. E. Harriman, *Chem. Phys. Lett.* **382**, 142 (2003).
- [17] J. Cioslowski and K. Pernal, *J. Chem. Phys.* **111**, 3396 (1999).
- [18] E. H. Lieb and S. Oxford, *Int. J. Quantum Chem.* **19**, 427 (1981).
- [19] J. P. Perdew, Y. Wang, *Phys. Rev. B* **45**, 13244 (1992).
- [20] D. M. Ceperley and B. J. Alder, *Phys. Rev. Lett.* **45**, 566 (1980).
- [21] G. Ortiz, P. Ballone, *Phys. Rev. B* **50**, 1391 (1994); **56**, 9970 (1997).
- [22] P. Gori-Giorgi and P. Ziesche, *Phys. Rev. B* **66**, 235116 (2002).